

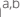











# Iron regulates the quiescence of naive CD4 T cells by controlling mitochondria and cellular metabolism

Ajay Kumar<sup>a,1,2</sup> , Chenxian Ye<sup>a,1</sup> , Afia Nkansah<sup>a,b</sup> , Thomas Decoville<sup>a</sup>, Garrett M. Fogo<sup>c</sup> , Peter Sajjakulnukit<sup>d</sup>, Mack B. Reynolds<sup>e</sup> , Li Zhang<sup>d</sup>, Osbourne Quayle<sup>b</sup> , Young-Ah Seo<sup>e</sup> , Thomas H. Sanderson<sup>c,f</sup> , Costas A. Lyssiotis<sup>d,f,g</sup> , and Cheong-Hee Chang<sup>a,2,3</sup> 

Edited by Kristin Hogquist, University of Minnesota Medical School Twin Cities, Minneapolis, MN; received October 29, 2023; accepted March 14, 2024

In response to an immune challenge, naive T cells undergo a transition from a quiescent to an activated state acquiring the effector function. Concurrently, these T cells reprogram cellular metabolism, which is regulated by iron. We and others have shown that iron homeostasis controls proliferation and mitochondrial function, but the underlying mechanisms are poorly understood. Given that iron derived from heme makes up a large portion of the cellular iron pool, we investigated iron homeostasis in T cells using mice with a T cell-specific deletion of the heme exporter, *FLVCR1* [referred to as knockout (KO)]. Our finding revealed that maintaining heme and iron homeostasis is essential to keep naive T cells in a quiescent state. KO naive CD4 T cells exhibited an iron-overloaded phenotype, with increased spontaneous proliferation and hyperactive mitochondria. This was evidenced by reduced IL-7R and IL-15R levels but increased CD5 and *Nur77* expression. Upon activation, however, KO CD4 T cells have defects in proliferation, IL-2 production, and mitochondrial functions. Iron-overloaded CD4 T cells failed to induce mitochondrial iron and exhibited more fragmented mitochondria after activation, making them susceptible to ferroptosis. Iron overload also led to inefficient glycolysis and glutaminolysis but heightened activity in the hexosamine biosynthetic pathway. Overall, these findings highlight the essential role of iron in controlling mitochondrial function and cellular metabolism in naive CD4 T cells, critical for maintaining their quiescent state.

heme | tonic signaling | iron | mitochondria

Activated CD4 T cells proliferate and differentiate into effector cells capable of producing cytokines to combat the tumor or pathogen-infected cells. Naive CD4 T cells receive T cell receptor (TCR) signaling through interactions with self-major histocompatibility complexes (MHC) presenting peptides (pMHC). While scanning the peripheral lymphoid organs, the TCRs of naive T cells briefly engage with self-pMHC (1, 2), providing sub-threshold impulses for the survival of naive T cells, as opposed to traditional TCR signaling and T cell activation. Upon activation, T cells undergo metabolic reprogramming accompanied by dynamic changes in cellular properties, including iron regulation. We have shown that tight control of iron homeostasis machinery is critical for T cell proliferation and mitochondrial functions (3). In addition, iron plays a role in the differentiation of proinflammatory CD4 T cells and is closely linked to glucose metabolism (4). Alterations in iron metabolism impact mitochondrial characteristics in T cells (4, 5), suggesting a significant interplay between iron homeostasis and T cell metabolism.

Iron plays a crucial role in many essential cellular functions, but its reactive nature makes it potentially cause oxidative damage if not properly regulated. To maintain the delicate balance between iron supply and demand, various regulatory mechanisms come into play, including iron uptake, usage, storage, and export (6). Dietary iron is absorbed in the intestine and transferred into the bloodstream via transferrin (Tf) molecules. Tf-bound iron enters the cell by binding to Tf receptor 1 (TfR1) on clathrin-coated pits (6). T cells increase surface expression of TfR1 (7) and take up non-Tf-bound iron after activation (8, 9). Missense mutations in the *TfR1* gene *TFRC* result in immunodeficiency (10) and faulty T cell proliferation (11), underlining the importance of iron flux and TfR1 expression in T cell biology. Free iron within the cytosol is known as the labile iron pool (LIP), which is available for use in cellular processes. However, excess amounts of unbound labile iron cause cellular damage through oxidative stress, mitochondrial damage, and ferroptosis. To prevent iron-induced damage, cells store excess iron in ferritin, a protein complex that sequesters iron within its core, and export excess iron through ferroportin (Fpn) (12).

In addition to free iron, a significant portion of iron is recycled from heme (13). Heme, an iron-containing porphyrin functions as a cofactor in a wide array of cellular processes (14). Heme is critical for mitochondrial oxidative phosphorylation, and heme deficiency

## Significance

Iron plays a crucial role in several physiological processes, including oxygen transport, DNA synthesis, mitochondrial function, and redox reactions. We have previously demonstrated that iron plays a critical role in the activation and proliferation of CD4 T cells. Iron overload leads to numerous immunological abnormalities, such as T cell dysfunction, but the mechanisms remain unclear. Here, our findings reveal that proper iron regulation is crucial for maintaining the quiescence and subsequent activation-induced proliferation of naive, but not effector, CD4 T cells. Using an iron-overloaded mouse model, we demonstrate that iron controls mitochondrial integrity and function in these cells. Moreover, the metabolic pathways are disrupted in iron-overloaded CD4 T cells, favoring the hexosamine biosynthetic pathway over glycolysis and glutaminolysis.

Competing interest statement: In the past 3 y, C.A.L. has consulted for Astellas Pharmaceuticals, Odyssey Therapeutics, Third Rock Ventures, and T-Knife Therapeutics, and is an inventor on patents pertaining to Kras regulated metabolic pathways, redox control pathways in pancreatic cancer, and targeting the GOT1-ME1 pathway as a therapeutic approach (US Patent No: 2015126580-A1, 05/07/2015; US Patent No: 20190136238, 05/09/2019; International Patent No: WO2013177426-A2, 04/23/2015).

This article is a PNAS Direct Submission.

Copyright © 2024 the Author(s). Published by PNAS. This article is distributed under [Creative Commons Attribution-NonCommercial-NoDerivatives License 4.0 \(CC BY-NC-ND\)](https://creativecommons.org/licenses/by-nc-nd/4.0/).

<sup>1</sup>A.K. and C.Y. contributed equally to this work.

<sup>2</sup>A.K. and C.-H.C. contributed equally to this work.

<sup>3</sup>To whom correspondence may be addressed. Email: [heechang@umich.edu](mailto:heechang@umich.edu).

This article contains supporting information online at <https://www.pnas.org/lookup/suppl/doi:10.1073/pnas.2318420121/-/DCSupplemental>.

Published April 15, 2024.

impairs the assembly of the electron transport chain subunits (15, 16). Heme synthesis is regarded as a generic housekeeping function that occurs in all cells, including T cells (17). Cells produce heme endogenously from de novo synthesis or take up exogenous heme through Feline Leukemia Virus subgroup C Receptor 2 (18). Heme production is tightly controlled by heme synthesis, degradation, and export (19). Alteration of these pathways leads to an imbalance in heme as well as iron homeostasis. The only known physiological mechanism of heme degradation in vertebrates is performed by heme oxygenase 1 (HO-1) (20). Once internalized, heme is catabolized by HO-1 to produce iron, biliverdin, and carbon monoxide or exported via FLVCR1, a known heme exporter (21). The role of heme in CD4 T cells is not well understood except that the levels of heme control T cell development and maintenance as demonstrated in FLVCR1 deficient mice (22). T cell-specific deletion of FLVCR1 showed normal development of T cells but their maintenance in the periphery is severely impaired.

Mitochondria is a hub of several metabolic processes beyond ATP generation. This includes the biosynthesis of iron-sulfur clusters and the regulation of heme and iron balance (16, 23). Iron is trafficked into mitochondria when required for metabolic purposes. Transport of iron across the inner mitochondrial membrane is known to be facilitated by the proteins mitoferrin 1 (MFRN1) and mitoferrin 2 (MFRN2), which are expressed in sites of erythropoiesis and ubiquitously, respectively (24). Importantly, optimal mitochondrial activity is critical for T cell activation and proliferation (25, 26). Mitochondrial function and its morphology, also known as mitochondrial dynamics, are closely connected. Mitochondria change their morphology to regulate and optimize the functionality (27, 28). These morphological changes involve fission and fusion, forming a dynamic network to maintain mitochondrial abundance, morphology, and cell function (29–31).

In this study, we report that naive CD4 T cells from FLVCR1-deficient mice exhibit elevated heme and iron, which resulted in spontaneous activation of naive but not effector/memory CD4 T cells. Upon activation, FLVCR1-deficient naive CD4 T cells

showed poor proliferation and increased ferroptosis. These defects were correlated with dysfunctional mitochondria and remodeling of cellular metabolism.

## Results

**Increased Intracellular Iron Stores in Knockout (KO) Naive CD4 T Cells.** We previously reported that iron plays an essential role in T cell activation and proliferation (3). Given that heme contributes to 95% of the iron in the human body, it strongly suggests that heme is closely involved in T cell responses. To gain a better understanding of how T cells regulate heme homeostasis, we first measured the heme contents of CD4 T cells during activation. The heme levels were decreased upon stimulation (Fig. 1A), which is similar to the reduction of iron in activated T cells (3). Our findings revealed that the mRNA expression of heme export protein FLVCR1 increased in activated CD4 T cells, peaking 1 d after activation and gradually declining thereafter (Fig. 1B). Loss of heme could be due to the export of heme or degradation by HO-1, as HO-1 levels were induced in activated T cells (Fig. 1C and *SI Appendix, Fig. S1A*).

To study the role of FLVCR1 in T cells in depth, we used mice with T cell-specific deletion of FLVCR1 (FLVCR1<sup>fl/fl</sup> CD4<sup>Cre</sup>, referred to as KO) as previously reported (22). Consistent with the previous study, the frequencies of T cells in the spleen were reduced in the KO mice (*SI Appendix, Fig. S1B*). The decrease in the T cell numbers was specific to naive T cells (CD62L<sup>hi</sup>CD44<sup>lo</sup>) as the numbers of effector T cells (CD62<sup>lo</sup>CD44<sup>hi</sup>) remained comparable to WT (*SI Appendix, Fig. S1C*). We hypothesized that FLVCR1 deletion disrupts the iron or heme homeostasis of naive T cells. To test the hypothesis, we measured the levels of heme and HO-1 in WT and KO naive CD4 T cells. Heme and HO-1 levels were comparable between WT and KO cells (Fig. 1D and *SI Appendix, Fig. S1D*). However, KO naive CD4 T cells had greater amounts of total iron compared to WT naive CD4 T cells, suggesting that release of heme-bound iron drove iron accumulation (Fig. 1E). The cytosolic free iron was similar between WT

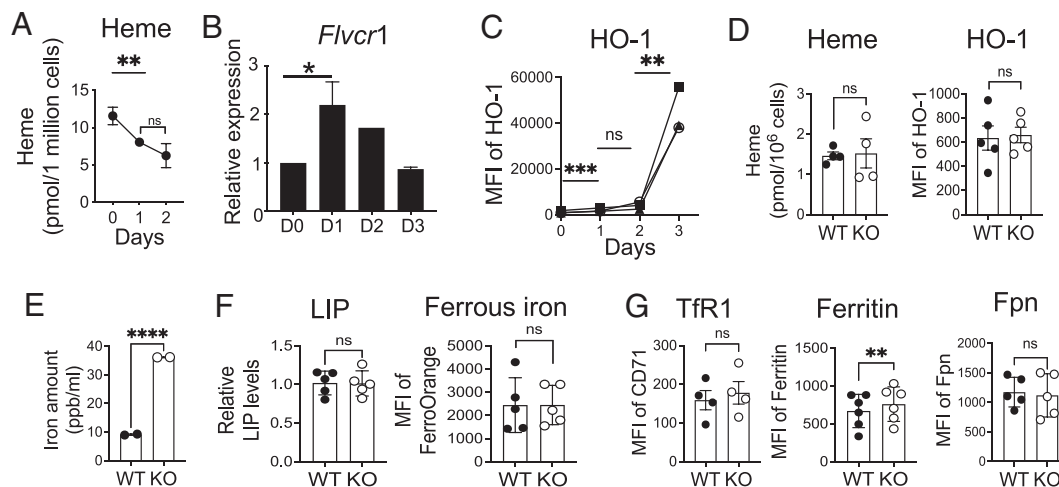


**Fig. 1.** Increased intracellular iron in FLVCR1 KO naive CD4 T cells. (A–C) Enriched naive CD4 T cells from C57BL/6 mice were activated with anti-CD3 and anti-CD28 antibodies as described in *Materials and Methods*. (A) Total cell lysate at indicated time points after stimulation and unstimulated (D0) cells were used to measure intracellular heme levels ( $n = 3$ ). (B) RNA was isolated from naive CD4 T cells at indicated time points and used for gene expression analysis using qPCR. A bar graph represents the relative gene expression of FLVCR1 ( $n = 3$ ). (C) HO-1 protein expression was measured by flow cytometry, and the mean fluorescence intensity (MFI) was shown ( $n = 3$ ). (D and E) Naive CD4 T cells from WT and KO mice were sorted and analyzed for the indicated parameters. (D) Graphs show the heme (Left) and HO-1 levels (Right) in naive CD4 T cells ( $n = 4$  to 5). (E) Total cell lysate was prepared from naive CD4 T cells and subjected to ICP-MS analysis. The graph shows the total iron level (reported in parts per billion per  $1 \times 10^6$  cells) ( $n = 2$ ). (F and G) Naive CD4 T cells (CD62L<sup>hi</sup>CD44<sup>lo</sup>) in total splenocytes were analyzed for the indicated parameters. (F) Graphs show the LIP measured using Calcein staining (Left) ( $n = 5$ ) and ferrous iron with FerroOrange (Right) ( $n = 5$ ). (G) Levels of Tfr1, ferritin, and Fpn were compared by flow cytometry. Graphs show MFI of Tfr1 ( $n = 4$ ), ferritin ( $n = 6$ ), and Fpn ( $n = 5$ ) in naive CD4 T cells. The data are the cumulative result of at least three independent experiments. Error bars represent the mean  $\pm$  SEM. \* $P < 0.05$ , \*\* $P < 0.01$ , \*\*\*\* $P < 0.0001$ , ns: not significant.

and KO naive CD4 T cells (Fig. 1*F* and *SI Appendix*, Fig. S1*E*). The expression of iron import protein (TfR1) and export (Fpn) proteins were maintained at comparable levels, whereas ferritin expression was higher in KO compared to WT CD4 T cells (Fig. 1*F* and *G* and *SI Appendix*, Fig. S1*F*). Together, KO naive CD4 T cells exhibited an iron-overload phenotype with the excess amount of iron stored in ferritin to avoid iron-mediated toxicity.

**FLVCR1 Deletion Alters the Homeostasis of Naive CD4 T Cells.** As FLVCR1 deletion primarily affects the naive T cell population, we asked whether FLVCR1 regulates naive T cell homeostasis in vivo. It is well established that the number of peripheral naive T cells remains constant through a balance of cell loss and regeneration (32). Therefore, we asked whether the loss of CD4 T cells in KO mice was due to the increased apoptosis of naive CD4 T cells. We found that naive CD4 T cells from the KO mice showed similar frequencies of apoptosis-mediated cell death compared to WT mice (Fig. 2*A*). Instead, KO naive CD4 T cells showed enhanced cell proliferation as measured by Ki-67<sup>+</sup> cells (Fig. 2*B*, *Left* and *SI Appendix*, Fig. S2*A*). BrdU labeling data further supported the increased proliferation of naive CD4 T cells in KO mice compared to WT (*SI Appendix*, Fig. S2*B*). However, no significant differences

in cell proliferation were observed in splenic effector CD4 T cells and also in thymic CD4 single-positive cells (Fig. 2*B*, *Middle* and *Right*), suggesting extrinsic signals from the periphery control KO naive CD4 T cell responses.

Without antigen challenges, naive T cell homeostasis is tightly controlled by TCR signaling. In addition, cytokine signaling through the IL-7 receptor (CD127) and IL-15 receptor (CD122) is crucial for not only the development but also the survival of T cells (33, 34). Therefore, we measured CD122 and CD127 expressions on both WT and KO naive splenic and thymic CD4 T cells. The expression of CD122 and CD127 was decreased on KO splenic naive CD4 T cells but not in thymic CD4 single-positive cells (Fig. 2*C* and *SI Appendix*, Fig. S2*C*), suggesting that naive CD4 T cells are not getting enough survival signal in the periphery. Naive T cells constitutively experience weak TCR stimulation in response to pMHC in the periphery, termed tonic signaling, which promotes T cell survival and maintenance (35). The expression of CD5 and Nur77 is directly proportional to self-ligand reactivity and TCR signaling strength (36, 37). We observed increased expression of CD5 and Nur77 in KO compared to WT CD4 T cells in the spleen but not in the thymus (Fig. 2*D* and *SI Appendix*, Fig. S2*D*). The expression of downstream signaling molecules including pERK, NF-κB, pSTAT5,

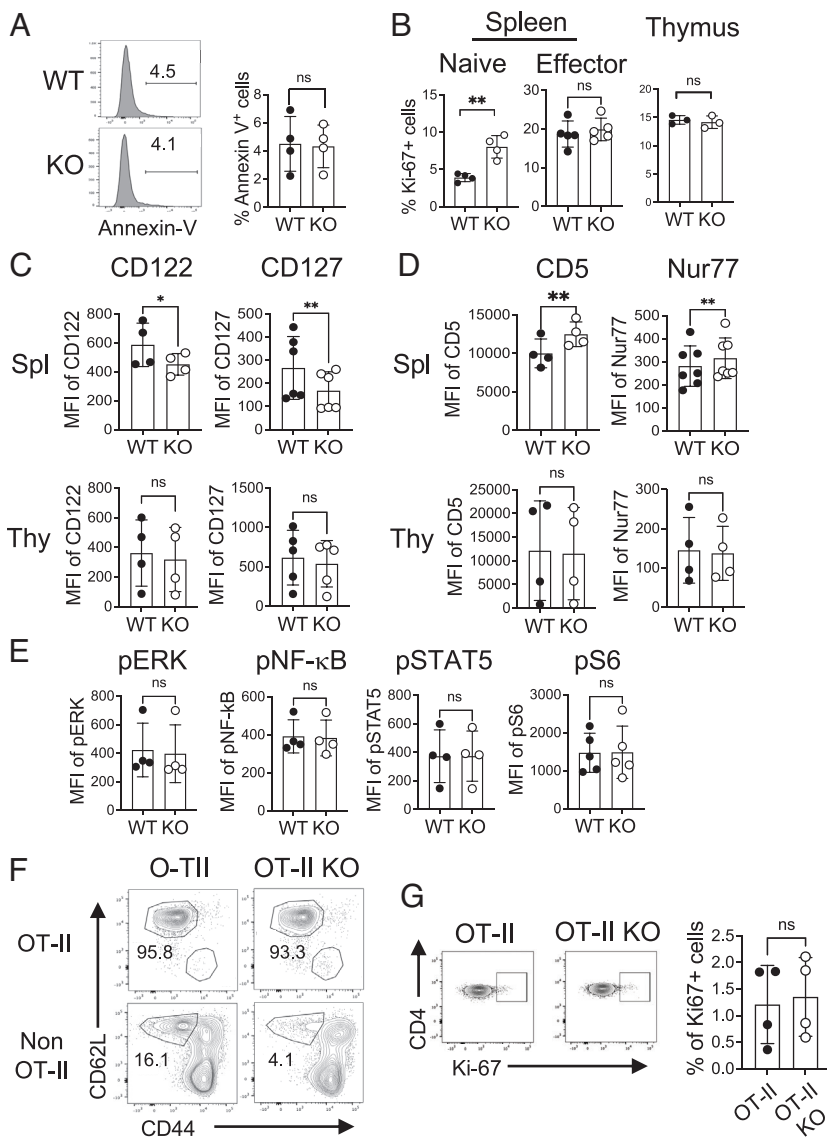


**Fig. 2.** FLVCR1 deletion alters the homeostasis of naive CD4 T cells. (A) Naive CD4 T cells in total splenocytes were examined for Annexin V. The representative histograms and the bar graph show % Annexin V<sup>+</sup> naive CD4 T cells from WT and KO mice (n = 4). (B) Graphs show percentages of Ki-67<sup>+</sup> in splenic naive (Left), and effector CD4 T cells (Middle), and single positive CD4 T cells from the thymus (Right) (n = 3 to 5). (C and D) Graphs show the expression of IL-7Ra (CD127) and IL-15R (CD122) (C), and CD5 and Nur77 (D) in naive CD4 T cells. The Top and Bottom panels show cells from the spleens and thymus, respectively (n = 4 to 7). (E) Total splenocytes from WT and KO mice were subjected to intracellular staining for the signaling molecules pERK, pNF-κB, pSTAT5, and pS6. Graphs show the expression of these signaling molecules in naive CD4 T cells (n = 4). (F and G) Total splenocytes from OT-II and OT-II KO mice were analyzed for the distributions of naive and effector CD4 T cells. (F) The representative dot plots show the percentages of naive and effector CD4 T cells in OT-II (Va2<sup>+</sup> Vb5<sup>+</sup>) and non-OT-II (Va2<sup>-</sup> Vb5<sup>-</sup>) CD4 T cells from OT-II and OT-II KO mice (n = 4). (G) Dot plots and the graph show percentages of Ki-67<sup>+</sup> naive CD4 T cells in the spleen (n = 4). The data are representative of at least three independent experiments. Error bars represent the mean ± SEM. \*P < 0.05, \*\*P < 0.01, ns: not significant.



and pS6 was comparable between KO and WT naive CD4 T cells (Fig. 2E and *SI Appendix, Fig. S2E*). Together, it seems that, in KO mice, naive CD4 T cells that received stronger tonic signaling survived while those weak signaling died in vivo.

To further investigate whether tonic signaling is responsible for poor survival of KO naive CD4 T cells, we utilized the TCR transgenic OT-II system. CD4 T cells in OT-II mice express V $\alpha$ 2 and V $\beta$ 5 TCR transgenes and recognize ovalbumin (Ova) in the context of MHC class II I-A<sup>b</sup> (38). Unlike polyclonal naive CD4 T cells with a range of tonic signaling, monoclonal naive CD4 T cells have the same affinity to self-antigens, in turn generating the same strength of tonic signaling. We hypothesized that FLVCR1 deletion would not affect OT-II naive T cells due to the same tonic signaling. We crossed KO mice with OT-II mice, generating FLVCR1-deficient OT-II mice (OT-II KO). The thymic selection of TCR transgenic cells is leaky, producing a CD4 T cell population expressing monoclonal OT-II TCR and polyclonal non-OT-II TCR (39). This allowed us to examine the potential differences in tonic signaling between two naive CD4 T cell populations in the same mouse. We found that the frequencies of OT-II KO naive CD4 T cells identified with V $\alpha$ 2<sup>+</sup> and V $\beta$ 5<sup>+</sup> TCR were similar to WT, whereas non-OT-II naive CD4 T cells (V $\alpha$ 2<sup>-</sup> and V $\beta$ 5<sup>-</sup>) were decreased in OT-II KO mice (Fig. 2F). Furthermore, OT-II KO naive CD4 T cells showed little difference in proliferation compared to WT naive OT-II T cells (Fig. 2G). In line with this finding, there was no difference in CD122 and CD127 expression levels between OT-II WT and KO naive CD4 T cells (*SI Appendix, Fig. S2F*). Together, FLVCR1 controls naive T cell homeostasis through TCR and IL-7/IL-15 signaling.

**Iron Overload Is Detrimental to Naive CD4 T Cells in Response to TCR Stimulation.** As we observed that KO naive CD4 T cells show hyperproliferation in vivo, we then investigated how KO naive T cells respond to subsequent in vitro activation. Activated KO CD4 T cells exhibited higher heme but not HO-1 levels than WT CD4 T cells (Fig. 3A). In addition, KO CD4 T cells had more LIP and ferrous iron than WT, which was accompanied by reduced iron import through TfR1 and increased storage in ferritin (Fig. 3B and C and *SI Appendix, Fig. S3A and B*). Similar levels of Fpn suggested that iron export was not affected in KO CD4 T cells (Fig. 3C and *SI Appendix, Fig. S3B*). These findings collectively indicated that KO CD4 T cells failed to regulate iron or heme homeostasis upon stimulation. Increased iron resulted in more cell death by apoptosis as the proportion of Annexin V<sup>+</sup> cells was increased in KO CD4 T cells (Fig. 3D). Excessive labile iron and heme can potentially lead to ferroptosis, an iron-dependent form of cell death (40, 41). Indeed, we found that KO CD4 T cells are more prone to ferroptosis than WT, as indicated by the ratio of green to red fluorescence measuring the lipid peroxidation in ferroptosis (Fig. 3E and *SI Appendix, Fig. S3C*). Ferroptosis of KO cells was reduced when a pharmacological inhibitor of ferroptosis was provided (*SI Appendix, Fig. S3D, Left*), but the inhibition was inefficient compared to WT cells (*SI Appendix, Fig. S3D, Right*). Overall, upon activation, iron-overloaded CD4 T cells undergo elevated cell death by apoptosis and ferroptosis.

Next, we assessed the proliferative responses of naive CD4 T cells from WT and KO mice in vitro. Although KO naive CD4 T cells displayed hyperproliferation in vivo, they had significant defects in proliferation when subjected to stimulation (Fig. 3F). In contrast, effector CD4 T cells activated in vitro showed no measurable difference in their proliferation (*SI Appendix, Fig. S3E*). The reduced cell proliferation was associated with decreased IL-2 production, measured by both intracellular IL-2 expression and secreted IL-2 in the media (Fig. 3G). Although the naive OT-II cell population

remained intact in OT-II KO mice, these cells proliferated poorly with lower frequencies of IL-2-expressing cells when stimulated (Fig. 3h and I). Similar to polyclonal naive CD4 T cells in KO mice shown in Fig. 3B, activated OT-II KO CD4 T cells displayed higher LIP levels (*SI Appendix, Fig. S3F*). Together, while the frequency of naive cells in OT-II KO mice was not affected in vivo, iron-overloaded OT-II CD4 T cells exhibited poor responses upon activation, separating the distinctive effect of high iron on the maintenance of naive cells and the proliferative capacity.

Poor IL-2 production prompted us to examine IL-2R (CD25) signaling. The expression levels of CD25 were not different between the WT and KO cells (Fig. 3J), but phosphorylation of STAT5 (pSTAT5) (Fig. 3K, Upper) was reduced in KO CD4 T cells after activation, suggesting weak IL-2R signaling in KO CD4 T cells. mTORC1 activation was not compromised, as evidenced by similar levels of pS6 in KO compared to WT CD4 T cells (Fig. 3K, Lower). KO cells also had comparable size and granularity to WT cells. (*SI Appendix, Fig. S3G*). We also observed a similar induction of pERK between WT and KO (*SI Appendix, Fig. S3H*), suggesting that the defect seems to be specific to IL-2R-mediated, not global signaling pathways. This was further supported since supplementing exogenous IL-2 did not rescue the defects (*SI Appendix, Fig. S3I*). Together, iron overload by FLVCR1 deletion impairs CD4 T cell proliferation by reducing IL-2/IL-2R signaling.

**Mitochondrial Fitness and Function Are Compromised in Iron-Overloaded CD4 T Cells.** Iron is actively involved in heme biogenesis and iron-sulfur protein assembly, which is essential for mitochondrial fitness and function (23). As we observed an iron overload phenotype of KO CD4 T cells, we asked how FLVCR1 deletion affects mitochondrial fitness and function. First, we measured the amount of iron in the mitochondria of WT and KO CD4 T cells using the fluorescent dye MitoFerroGreen (MFG), which specifically detects iron in mitochondria (42). In contrast to LIP, which is downregulated (3), mitochondrial iron increased after activation, suggesting that iron is translocated from the cytoplasm and/or generated in mitochondria upon TCR stimulation (Fig. 4A and *SI Appendix, Fig. S4A*). This was not due to the activation-induced increase in mitochondrial mass (MM) as the ratio of mitochondrial iron over mass was also increased (*SI Appendix, Fig. S4B*). KO naive CD4 T cells before activation had higher levels of mitochondrial iron than WT, but the levels were not induced in activated KO cells (Fig. 4B and *SI Appendix, Fig. S4C*). The mitochondrial protein mitoNEET (mtNEET) (gene *cisd1*) is a redox-sensitive iron-sulfur protein that helps export iron-sulfur molecules out of mitochondria into the cytosol, thus a powerful regulator of mitochondrial iron content (43). We found that levels of mtNEET in KO cells were lower before activation (D0), but higher after activation (D2) than in WT cells (Fig. 4C). The results may explain that lower levels of mtNEET in KO CD4 T cells facilitate the retention of mitochondrial iron before activation, while higher levels of mtNEET after activation release more iron from the mitochondria, inducing inefficient mitochondrial iron accumulation in activated KO CD4 T cells.

Mitochondria are highly dynamic organelles and maintain their morphology via constant processes of fission and fusion (44). As reported, iron homeostasis is closely associated with mitochondrial morphology and size (45). A study has shown that mitochondrial dynamics are different between effector and memory CD8 T cells (46) but how naive CD4 T cells control mitochondrial biogenesis upon activation has not been studied. To investigate this, we performed microscopy to compare the morphology and size of

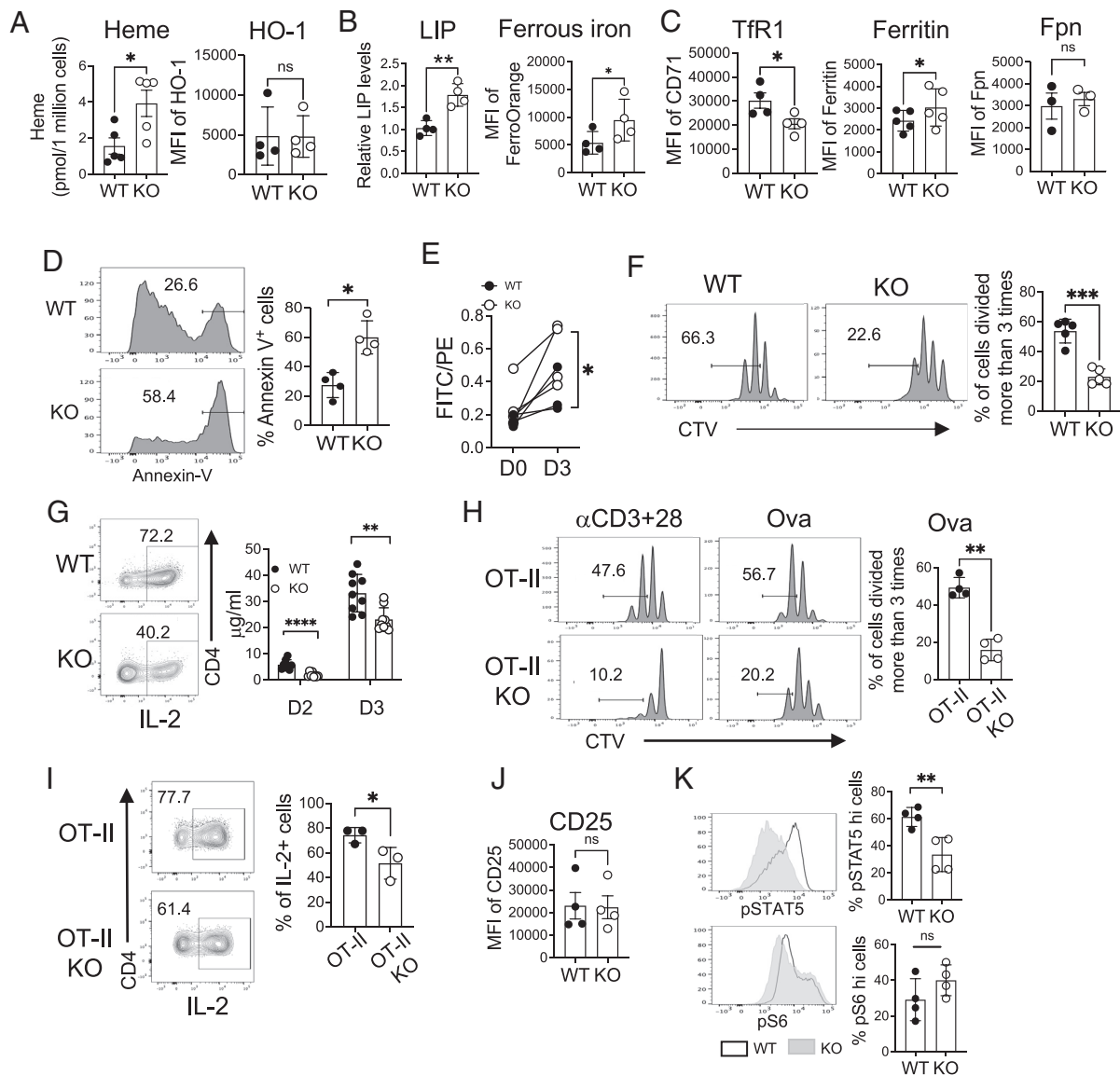


**Fig. 3.** Iron overload is detrimental to naive CD4 T cells in response to TCR stimulation. Sorted naive CD4 T cells from the spleens of WT and KO mice were labeled with CellTrace™ Violet (CTV) and then activated with anti-CD3 and anti-CD28 antibodies for 3 d as described in *Materials and Methods*. (A) Graphs show levels of heme (Left) and HO-1 (Right) in activated CD4 T cells (n = 4 to 5). (B and C) The graphs show the expression of the indicated parameters (n = 3 to 5). (D) The representative histograms and the summary graph show the percentages of Annexin V<sup>+</sup> in activated CD4 T cells from WT and KO mice (n = 4). (E) Cells were stained with a lipid-peroxidation reagent. The graph shows the ratio of fluorescence intensity of FITC over PE. (F) The representative histograms and the summary graph show cell proliferation (n = 5). (G) Cells were stimulated with PMA and ionomycin for 4 h and then analyzed for intracellular IL-2 expression. Representative dot plots show the percentage of IL-2<sup>+</sup> CD4 T cells (n = 3). The summary graph shows the amount of IL-2 secreted into the media at indicated time points as measured by ELISA (n = 9). (H) Enriched naive CD4 T cells from OT-II and OT-II KO mice were stimulated with dendritic cells in the presence of 100 mg/mL of Ova protein for 3 d. Cells were also activated with anti-CD3 and anti-CD28 antibodies. The representative histograms depict cell proliferation (n = 4). (I) Cells in (H) were restimulated with PMA and ionomycin for 4 h and then assessed for the expression of IL-2 cytokine. Representative dot plots and the summary graph show the percentages of IL-2<sup>+</sup> OT-II CD4 T cells (n = 3). (J) The graph shows CD25 expression in activated CD4 T cells (n = 4). (K) Activated CD4 cells were subjected to intracellular staining of pSTAT5 and pS6. The data are representative of three independent experiments. Error bars represent the mean ± SEM. \**P* < 0.05, \*\**P* < 0.01, \*\*\**P* < 0.001, ns: not significant.

mitochondria. We found that total mitochondrial volume increased in both WT and KO CD4 T cells after activation (Fig. 4D and *SI Appendix, Fig. S4D*). However, each mitochondrion in activated KO CD4 T cells was smaller and shorter than WT (Fig. 4E). This suggests that KO cells have more fragmented mitochondria, likely due to a higher fission rate than WT cells after activation. One of the proteins regulating the fission process is Drp1 and activated Drp1 by phosphorylation at serine 616 is brought from the cytosol to the mitochondrial surface to catalyze the fission process (47). We found that T cell activation induced the accumulation of activated pDrp1(S616) in WT cells (Fig. 4F, Left and *SI Appendix, Fig. S4E*), which promotes fission in

activated CD4 T cells. pDrp1(S616) levels were elevated in KO CD4 T cells compared to WT cells (Fig. 4F, Right), explaining higher mitochondrial fission of activated KO CD4 T cells.

Studies have shown that T cell effector functions are directly regulated by mitochondria (48), and iron deficiency has been strongly linked to mitochondrial dysfunction in T cells (3). Having observed the changes in mitochondrial iron in KO CD4 T cells, we asked whether iron overload affects mitochondrial functions. To answer this, we measured MM, membrane potential (MP), and reactive oxygen species produced in mitochondria (mROS). Our data revealed that KO naive CD4 T cells had higher levels of MM, MP, and mROS before stimulation (D0) (Fig. 4G

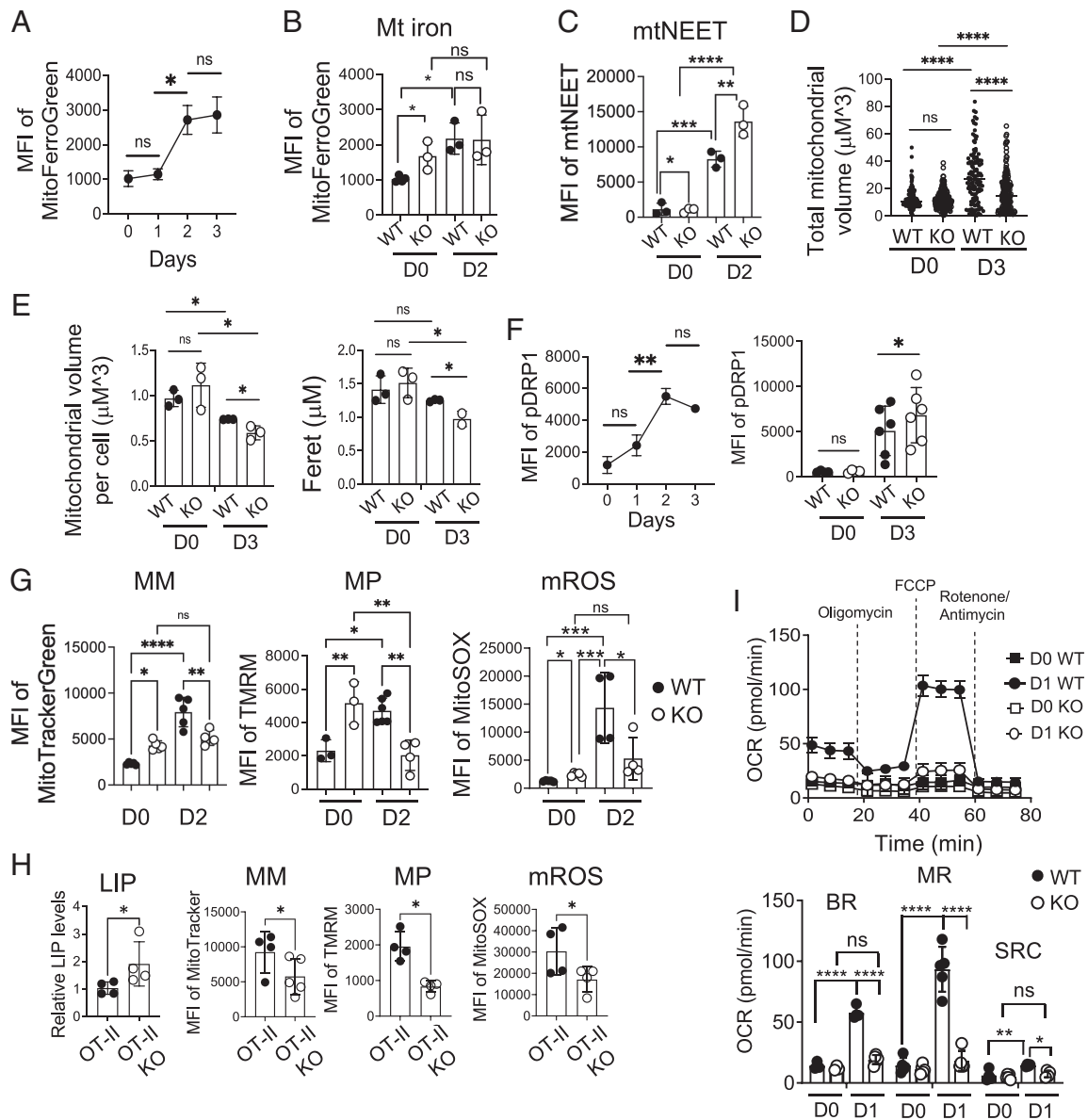


**Fig. 4.** Mitochondrial fitness and function are compromised in iron-overloaded CD4 T cells. (A) Enriched naive CD4 T cells from C57BL/6 mice were activated and analyzed for mitochondrial iron levels using MFG. The graph shows the MFI of MFG over time (n = 4). (B and C) Sorted naive CD4 T cells from WT and KO mice were activated for 2 d. Graphs show mitochondrial iron (B) and the expression of mtNEET (C) from unstimulated (D0) and stimulated (D2) CD4 T cells (n = 3). (D and E) Sorted naive CD4 T cells from WT and FLVCR1 KO mice were activated for 3 d. Unstimulated (D0) and stimulated cells (D3) were subjected to ATP synthase (ATPB) staining to mark mitochondria and DAPI for nuclei, followed by visualization via the Zeiss Axio Observer with multichannel LED illumination. Analysis of the mitochondrial volume and length was performed using a custom Fiji macro script. (D) The graph shows the total volume of mitochondria of WT and KO before and after activation (n = 2 to 3). (E) Graphs show the volume (Left) and the length (Right) of mitochondria. A total number of 661 cells were examined (n = 2 to 3). (F) Enriched WT and KO naive CD4 T cells were activated and analyzed for pDrp1 expression. The Left graph shows the MFI of pDrp1 over time (n = 3). The Right graph shows pDrp1<sup>Ser616</sup> expression in unstimulated (D0) and stimulated (D3) CD4 T cells from WT and KO mice (n = 4 to 6). (G) Sorted naive CD4 T cells from WT and FLVCR1 KO were activated for 2 d and subjected to MitoTracker, TMRM, and MitoSOX staining. The graphs show MFI values of MitoTracker, TMRM, and MitoSOX from unstimulated (D0) and stimulated cells (D2), depicting MM, MP, and mROS respectively (n = 3 to 5). (H) Enriched naive CD4 T cells from OT-II and OT-II KO mice were stimulated with dendritic cells in the presence of 100 mg/mL of Ova protein for 3 d. The graphs show LIP levels and MFI of MitoTracker green, TMRM, and MitoSOX (n = 4). (I) Naive CD4 T cells from WT and KO mice were activated for 1 d. The representative graph at the Top shows OCR using the Mito Stress Test in the Seahorse assay from unstimulated (D0) and stimulated cells (D1). The bar graph at the Bottom shows BR, maximum respiratory capacity (MRC), and reserve capacity (RC) (n = 6). The data are representative of at least three independent experiments. Error bars represent the mean ± SEM. \*P < 0.05, \*\*p < 0.01, \*\*\*p < 0.001, \*\*\*\*p < 0.0001, ns: not significant.

and *SI Appendix, Fig. S4F*). In contrast to naive cells before activation, these mitochondrial parameters were significantly reduced after activation (D2), which would contribute to poor proliferation (Fig. 4G and *SI Appendix, Fig. S4F*). However, there was little difference in effector CD4 T cells for these mitochondrial parameters (*SI Appendix, Fig. S4G*), suggesting different roles of FLVCR1 on naive vs. effector CD4 T cells. To explore whether these observed phenotypes are a result of in vitro culture conditions differing from those in vivo, we studied T cell activation in vivo

by administering anti-CD3 antibodies for a duration of 1 d. In line with our in vitro results, CD4 T cells in KO mice exhibited an activation defect, as evidenced by reduced CD69 expression and compromised mitochondrial MP (*SI Appendix, Fig. S4H and I*). KO mice also showed lower mitochondrial iron in activated CD4 T cells compared to the WT group (*SI Appendix, Fig. S4J*). We also examined mitochondria in OT-II and OT-II KO CD4 T cells. Unlike KO mice, CD4 T cells from OT-II KO mice did not show a measurable defect in mitochondrial functions before



activation (*SI Appendix, Fig. S4K*). However, OT-II KO cells showed increased LIP and poor mitochondrial responses upon activation (Fig. 4H), mirroring the observations in polyclonal KO CD4 T cells. To further study mitochondrial responses, cells were subjected to the mitochondria stress test using the Seahorse assay. The data showed that basal respiration (BR), maximum respiration, and spare respiratory capacity were enhanced upon activation of WT cells, but KO cells failed to show induction. Furthermore, KO cells did not show a significant elevation of mitochondrial function upon activation (Fig. 4I). In conclusion, these findings highlight the detrimental effects of high iron levels on mitochondrial dynamics and function in CD4 T cells.

#### Iron Controls Glucose and Glutamine Metabolism in CD4 T Cells.

A recent study revealing the impact of iron deprivation on glucose metabolism in CD4 T cells (4) prompted us to investigate the role of FLVCR1 in CD4 T cell glucose metabolism. When assessing glucose uptake using a fluorescent glucose analog (2-NBDG) and the expression of glucose transporter 1 (Glut1), we found that both were similar between activated WT and KO CD4 T cells (Fig. 5A). However, when cells were subjected to be examined for glucose metabolism using the Seahorse assay, we found that the extracellular acidification rate (ECAR) was greatly lower in KO than WT CD4 T cells, suggesting that iron overload compromised glycolysis in CD4 T cells (Fig. 5B). Given that glycolysis is critical for CD4 T cell proliferation, we explored whether inefficient glycolysis contributed to the observed reductions in cell proliferation and mitochondrial function. To test this, we supplemented KO naive CD4 T cells with sodium-lactate to fuel glycolysis during activation. We found that cell proliferation, IL-2 production, and mitochondrial MP were partially rescued in the presence of sodium-lactate (Fig. 5 C–E). These results support the hypothesis that iron overload drives inefficient glycolysis, ultimately leading to impaired proliferation and compromised mitochondrial functions. Together, our study underscores the pivotal role of iron in modulating glycolysis programs in CD4 T cells in response to TCR stimulation.

When glucose becomes limited, T cells have been shown to increase glutamine metabolism as a compensatory mechanism (49). Therefore, it is possible that T cells with iron overload attempt to meet their metabolic needs by elevating glutaminolysis. To test this, we measured the levels of amino acid transporter CD98 and found higher levels in activated KO CD4 T cells, which was correlated with increased amounts of glutamine compared to WT CD4 T cells (Fig. 5F and *SI Appendix, Fig. S5A*). Surprisingly, however, levels of glutamate and  $\alpha$ -ketoglutarate ( $\alpha$ KG), downstream metabolites of glutamine, were significantly lower in KO CD4 T cells than WT cells (Fig. 5F). Glutathione (GSH) did not show a significant difference (Fig. 5F). We asked whether supplementing  $\alpha$ KG to the culture medium could restore the proliferation of KO CD4 T cells. We found that additional  $\alpha$ KG failed to rescue proliferation of KO CD4 T cells (*SI Appendix, Fig. S5B*), indicating KO cells suffer from other metabolic deficits in addition to glutaminolysis. As increased glutamine by KO CD4 T cells did not accumulate glutamate and  $\alpha$ KG, we hypothesized that glutamine was being metabolized through an alternative pathway, such as the hexamine biosynthesis pathway (HBP), which is essential for modifying protein glycosylation. To test this, we evaluated the overall glycosylation of proteins by measuring uridine diphosphate N-acetylglucosamine (O-GlcNAc) expression and observed increased glycosylation in KO cells (Fig. 5 G, *Left* and *SI Appendix, Fig. S5 C, Left*). Additionally, the expression of ICAM-1, which relies on glycosylation for cell surface expression (50), was elevated in KO cells (Fig. 5 G, *Middle* and *SI Appendix, Fig. S5 C, Middle*).

L-PHA, a glycosylation marker, was also upregulated in KO cells (51, 52) (Fig. 5 G, *Right* and *SI Appendix, Fig. S5 C, Right*). Moreover, in vivo activation of CD4 T cells in KO mice also showed higher ICAM-1 expression after activation (*SI Appendix, Fig. S5D*) supporting the in vitro observations. Enhanced HBP in KO CD4 T cells prompted us to investigate whether iron directly regulates HBP by adding an iron chelator, deferoxamine (DFO), to WT cells during activation. DFO treatment did not affect mitochondrial iron, O-GlcNAc, or L-PHA (*SI Appendix, Fig. S5E*). Together, iron overload reduces glutaminolysis and does not seem to directly regulate HBP.

Because supplementing sodium-lactate to KO cells restored proliferation and IL-2 production, we asked whether glutamine and HBP metabolism would be corrected in these cells. We found that KO cells stimulated in the presence of sodium-lactate reduced the levels of CD98 to that of WT cells, but glutamine levels remained high (*SI Appendix, Fig. S5 F, Left* and *Middle*). Furthermore, glycosylation was further increased in the presence of sodium-lactate (*SI Appendix, Fig. S5 F, Right*). Together, sodium-lactate showed different effects on metabolism and did not restore glutamine or HBP metabolism in KO cells.

#### Iron Overload Remodels Metabolic Programming in Naive CD4 T Cells.

Since we identified a key role of FLVCR1 in regulating metabolic pathways, we sought to identify broader metabolic effects of iron overload. To this end, we performed a targeted metabolomics study to identify FLVCR1-dependent changes in metabolite levels. We observed distinct metabolic profiles, particularly related to central carbon metabolism, of KO naive CD4 T cells from WT cells before (D0) and after (D1) activation (*SI Appendix, Fig. S6A*). Pathway enrichment analyses revealed that the pathways uniquely presented by KO cells compared to WT cells are pyruvate metabolism, glycolysis, the pentose phosphate pathway, and nicotinate and nicotinamide metabolism (*SI Appendix, Fig. S6 B, Left*). After activation, KO CD4 T cells were enriched in purine metabolism and amino acid metabolism (*SI Appendix, Fig. S6 B, Right*).

Hierarchical clustering analysis showed increased amounts of several glycolytic metabolites, such as lactate and pyruvate, with FLVCR1 deficiency prior to activation (Fig. 6 A, *Left*). This indicates enhanced anabolic activities in the KO naive CD4 T cells. Furthermore, HBP metabolites, such as N-acetyl glucosamine 1-phosphate and Uridine 5-triphosphate, were lower in KO CD4 T cells, which suggests that HBP is dampened by elevated glycolysis in KO naive CD4 T cells. When cells were activated, glutamine and its derivative metabolites, such as tryptophan, as well as the oxidized form of glucose (gluconic acid), were increased in KO CD4 T cells, while oxidized glutathione and ATP were decreased (Fig. 6 A, *Right*). The data suggests that, in iron-overloaded CD4 T cells, glucose might not be efficiently metabolized to produce lactate or ATP.

Glucose-fueled metabolites such as dihydroxyacetone phosphate, phosphoenolpyruvate, and nicotinamide adenine dinucleotide (NAD) were significantly lower in activated KO CD4 T cells, while pyruvate was not significantly different (Fig. 6 B, *Top*). The pentose phosphate pathway metabolite, D-Ribose 5-phosphate pathway (PPP), was higher in KO cells, suggesting glucose might be fueling PPP in these cells. Glutamine, a critical component required for activation and proliferation of T cells, was higher in activated KO cells but was not efficiently metabolized to produce aspartate or supported HBP, despite producing higher ATP in KO cells (Fig. 6 B, *Bottom*). Together, iron overload in CD4 T cells through FLVCR1 deletion results in dysregulation of metabolic pathways, which have been previously demonstrated to govern activation.

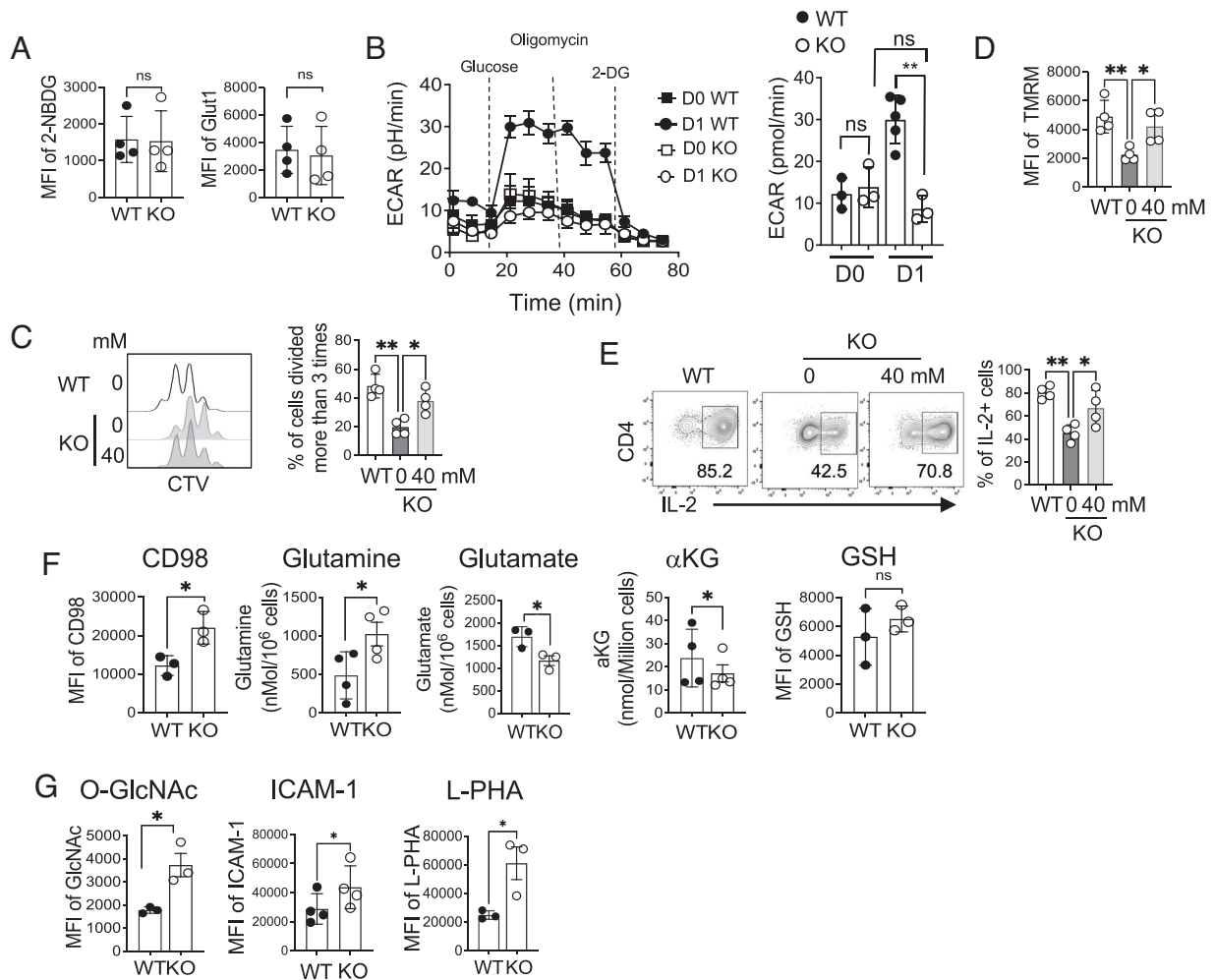


**Fig. 5.** Iron controls glucose and glutamine metabolism in CD4 T cells. (A) Sorted naive CD4 T cells from WT and KO mice were activated for 3 d and compared for 2-NBDG uptake (*Left*) and expression of Glut1 (*n* = 4). (B) Sorted naive CD4 T cells were activated for 1 d and subjected to the Seahorse assay. The representative graph on the *Left* shows ECAR using the glycolytic stress test from unstimulated (D0) and stimulated cells (D1). The bar graph on the *Right* shows glycolytic capacity (*n* = 6). (C–E) Sorted naive CD4 T cells from KO mice were stimulated for 3 d in the presence of sodium-lactate. (C) The representative histograms and graph show cell proliferation (*n* = 4). (D) The graph shows TMRM of activated CD4 T cells with or without sodium-lactate. (E) The same cells were restimulated with PMA and ionomycin for 4 h and then analyzed for IL-2 cytokine. (F and G) Sorted naive CD4 T cells from WT and KO mice were activated with anti-CD3 and anti-CD28 antibodies for 3 d and analyzed for the indicated parameters. The graphs in (F) show the MFI of CD98 and amounts of glutamine and glutamate, αKG, and GSH levels in activated CD4 T cells (*n* = 3 to 4). (G) Graphs show MFI of intracellular levels of O-GlcNAc modification, ICAM-1 on the cell surface, and L-PHA levels in activated CD4 T cells (*n* = 3 to 4). The data are representative of at least three independent experiments. Error bars represent the mean ± SEM. \**P* < 0.05, \*\**P* < 0.01, \*\*\**P* < 0.001, ns: not significant.

To further understand the effect of FLVCR1 on glucose metabolism, we performed glucose tracing experiments (highlighted by black circles in *SI Appendix*). KO cells showed reduced oxidation of <sup>13</sup>C-glucose through the TCA cycle into pyruvate and lactate (Fig. 6 C, *Top*). This reduced pyruvate production also led to inefficient entry of glycolytic pyruvate into the TCA cycle in KO cells, as indicated by the reduced production of various <sup>13</sup>C TCA cycle metabolites such as citrate, fumarate and malate (Fig. 6 C, *Middle*). We also observed, in KO cells, a reduced trend for glucose-derived carbon oxidation into glutamate and GSH but fueled more to UDP-GlcNAc (Fig. 6 C, *Lower*). These results are consistent with the findings shown in Fig. 5 that FLVCR1 deficiency affects glucose oxidation and that it's fueling glutamine metabolism to some extent.

## Discussion

The control of iron homeostasis links metabolic pathway activity to cell activation, proliferation, and survival, especially in T cells. A recent study highlighted the potential of altering iron

metabolism in T cells to mitigate the clinical symptoms of systemic lupus erythematosus (53). Therefore, it is crucial to understand how CD4 T cells use iron to proliferate and function in response to immunological challenges. In this study, we found that an excess of iron in naive CD4 T cells amplifies their sensitivity to tonic signaling, which in turn results in the hyperactivation of mitochondria and spontaneous proliferation. However, in response to activation, these naive CD4 T cells exhibited considerable defects in activation and proliferation, accompanied by an increase in ferroptosis and alterations in cellular metabolism. Additionally, we showed that the amount of iron in mitochondria accumulates during activation, which is compromised in CD4 T cells with iron overload.

Integration of several factors, including TCR signaling, costimulation, and cytokine guidance, is required for CD4 T cell activation. Naive T cells survey MHC presenting self-peptides and receive low-intensity tonic signaling in the absence of an immunological challenge (54). Such tonic signaling, while insufficient for actual activation, influences essential processes including basal signaling, gene expression, and metabolic activity (55). Iron



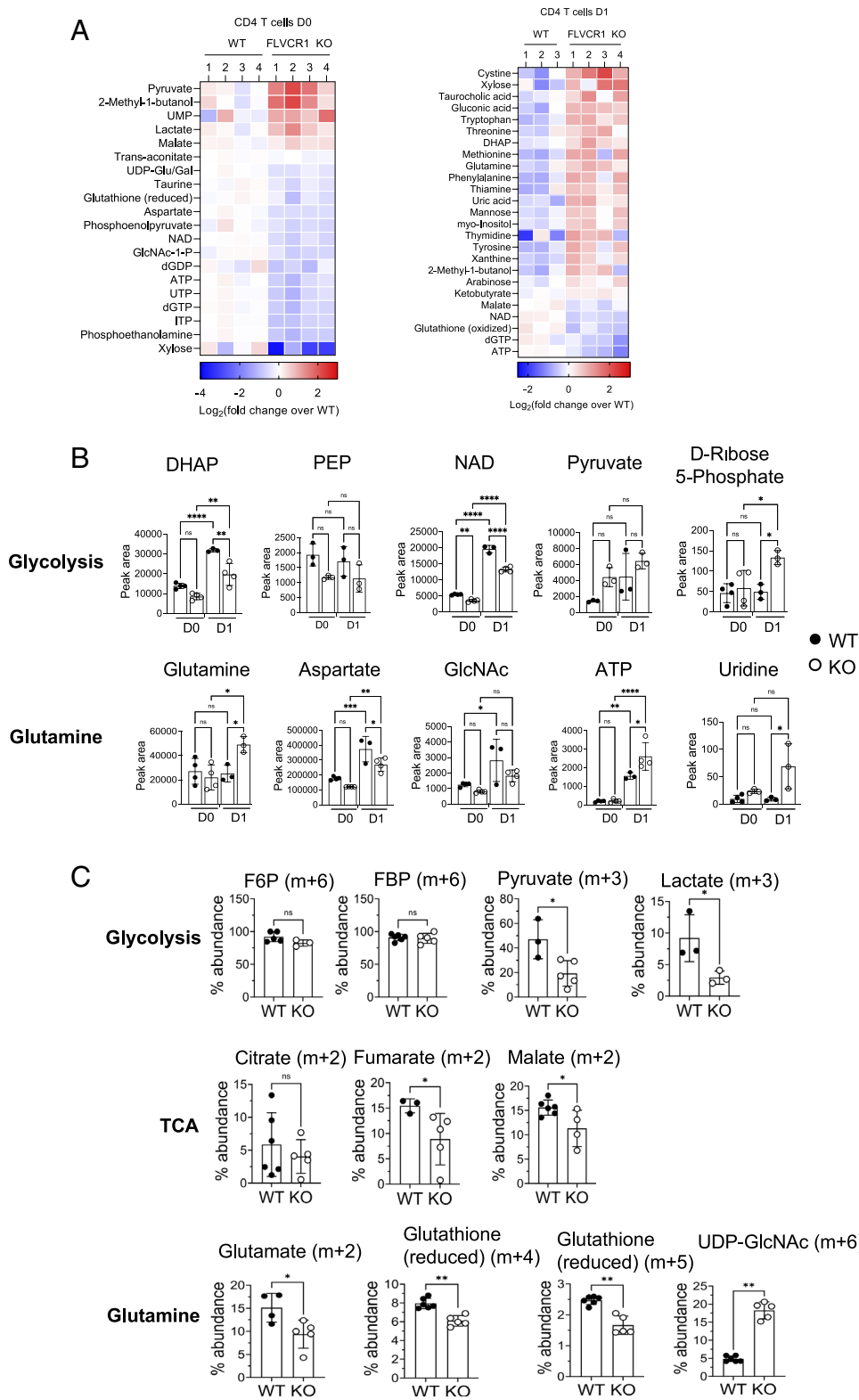


**Fig. 6.** Iron overload remodels metabolic programming in naive CD4 T cells. Sorted naive CD4 T cells from WT and KO mice were activated, and metabolites were extracted from unstimulated cells (D0) and stimulated cells (D1). Metabolite extracts were subjected to targeted metabolomic analysis using LC-MS/MS with a reference library of 230 metabolites. (A) Heat maps show significantly different amounts of metabolites between KO and WT naive CD4 T cells at D0 (Left) and D1 (Right) ( $n = 3$ ). (B) Graphs show relative levels of the indicated metabolites from glucose (Upper) and glutamine (Lower) metabolism pathways ( $n = 3$  to 4). (C) WT and KO naive CD4 T cells were stimulated for 1 d in glucose-free RPMI containing glutamine (2 mM) and [ $^{13}\text{C}_6$ ]-glucose (11 mM). After 1 d of activation, cell extract was prepared and subjected to LC-MS analysis. Representative graphs show the percentage abundance of [ $^{13}\text{C}_6$ ]-glucose-derived carbon in glycolysis (F6P, FBP, pyruvate, and lactate), TCA cycle (citrate, fumarate, and malate), glutamine metabolism (glutamate and GSH) and HBP (UDP-GlcNAc) intermediate metabolites. The error bars represent the mean  $\pm$  SEM. \* $P < 0.05$ , \*\* $P < 0.01$ , \*\*\* $P < 0.001$ , ns: not significant.

overload seems to change the sensitivity of naive CD4 T cells to these tonic signals, causing the cells to exit the quiescent state or die. The majority of naive CD4 T cells disappear in KO mice, which suggests that iron levels control tonic signaling and high iron leads to weak signaling driving death. Besides the degree of self-reactivity of naive T cells, cytokine signaling regulates CD4 T cell metabolism (56). Therefore, in addition to weak tonic signaling, the lack of adequate survival signaling is likely the underlying reason for the reduction of naive T cells in KO mice. A prior

work described that Foxo1 is essential for maintaining naive CD4 T cells by controlling the expression of IL-7R (57). While we cannot rule out the possibility that iron controls Foxo1, our data suggest that changes in mitochondrial properties due to excess iron led to poor survival.

A previous study suggests an inverse correlation between the degree of self-reactivity and T cell metabolism (58). In contrast to this, we observed that iron-overloaded CD4 T cells exhibited increased glycolysis before activation, followed by a substantial

decrease after stimulation. We observed that although supplementing lactate partially rescued the defects in KO CD4 T cells, it did not restore glutamine or HBP metabolism, indicating cell proliferation is likely associated with improved glycolysis. Furthermore, providing  $\alpha$ KG did not rescue the defects in KO CD4 T cells, suggesting other factors may also be involved. In line with this notion, the expression of the glycolytic enzymes hexokinase 2 and glyceraldehyde-3-phosphate dehydrogenase, along with the pyruvate dehydrogenase activity, is regulated by the transcription factor BTB and CNC homology 1 (BACH1) (59). Furthermore, heme is known to regulate the expression of both BACH1 and BACH2 (60, 61). BACH2 also is important for maintaining naive T cells in the periphery (62). Therefore, it is possible that changes to BACH2 expression in the absence of heme export could lead to the loss of naive T cells in KO mice.

It has been previously reported that the reduction in heme export leads to an increase in TCA-cycle fueling (63), which contrasts with our observations. The discrepancy could be attributed to at least two factors. First, we used primary naive CD4 T cells from KO mice, while the reported study utilized a siRNA approach with cancer cell lines. Second, the difference could be due to the targeted deletion of one isoform vs. both isoforms of FLVCR1. FLVCR1 has two isoforms: FLVCR1a and FLVCR1b. FLVCR1a is an exporter at the cell membrane (64), and FLVCR1b is responsible for heme export from the mitochondria (65). In our study, we employed a KO system where both isoforms were deleted, whereas the aforementioned study targeted only FLVCR1a. We hypothesize that blocking heme export from the mitochondria leads to severe defects in mitochondrial functionality and metabolic programming, as we demonstrated. However, T cells deficient in each isoform are currently unavailable, warranting further investigation to have a better understanding of the role of heme and iron in different compartments in T cells.

Iron metabolism is a tightly regulated process. Heme, as the main source of iron, is actively involved in the regulation of iron metabolism. The breakdown of heme by HO-1 releases free iron into the cytosol, as the induction of HO-1 elevates intracellular iron levels and modulates cytokine responses (66). It is reported that cells lacking FLVCR1a isoform attempt to downregulate heme synthetic pathways and upregulate heme degradation to prevent excess heme accumulation, resulting in increased iron levels with iron storage and export (64). Consequently, the metabolic pathways of iron and heme are intricately interconnected to regulate immune responses.

Iron-overloaded CD4 T cells attempt to reduce iron imports and store iron in ferritin to counteract the detrimental effects of excess iron. Although iron is essential for mitochondrial activity and mitochondria contribute to cellular iron metabolism, the mechanisms by which mitochondria obtain iron are still poorly understood. It is believed that several mechanisms exist, including the uptake of cytosolic iron (67) and the direct transfer of extracellular iron from endosomes to the mitochondria (68). Iron also plays a key role in producing iron-sulfur (Fe-S) clusters, which is one of the essential functions of mitochondria (69). These Fe-S molecules are exported via mtNEET, a Fe-S protein found on the outer mitochondrial membrane (69). Typically, mtNEET remains inactive when the Fe-S cluster is in a reduced state but is activated when a signal induces the cluster to oxidize (69, 70). Our findings showed enhanced mtNEET expression in iron-overloaded CD4 T cells after activation, suggesting an increase in the export of Fe-S molecules via mtNEET and a subsequent decrease in mitochondrial free

iron in these cells. Taken together, our findings underscore that both iron overload and iron deprivation conditions appear to inhibit mitochondrial respiration (4), thereby emphasizing the critical role of iron homeostasis in maintaining optimal mitochondrial functionality.

Metabolic dysregulation is widely known to increase the risk of developing both cancer and immune-related diseases (71). For example, in rheumatoid arthritis, the invasiveness of T cells within tissues has been linked to dysregulated mitochondrial activity and fatty acid metabolism (72). Conversely, heightened glycolysis and mitochondrial respiration have been observed in CD4 T cells from lupus patients (4). Our findings highlight the role of iron in maintaining mitochondrial integrity and metabolic balance in CD4 T cells. It would be valuable to investigate whether disruptions to iron homeostasis are present in patients suffering from cancer or autoimmune diseases.

## Conclusions

The deficiency of FLVCR1 results in iron overload, which consequently modifies the function and dynamics of mitochondria in naive CD4 T cells. Iron-overloaded naive, but not effector, CD4 T cells receive heightened tonic signaling, triggering an increased rate of spontaneous proliferation. However, iron-overloaded naive CD4 T cells respond poorly to activation stimuli and die of ferroptosis. This is at least partly contributed to dysregulated iron accumulation in the mitochondria and metabolic programming. Together, iron homeostasis is an essential player for maintaining quiescence and the survival of naive CD4 T cells. A more comprehensive understanding of the mechanisms of iron metabolism can potentially facilitate the development of innovative therapeutic treatments for patients suffering from iron overload.

## Materials and Methods

Complete experimental methods are described in *SI Appendix, Materials and Methods*.

FLVCR1<sup>fl/fl</sup> CD4<sup>Cre</sup> mice were generated in Abkowitz's laboratory. Flow cytometry analysis of murine tissues was undertaken on a BDFACSCanto or an LSRFortessa cell analyzer, and FACS data were analyzed using FlowJo v10. Sample preparation and antibody staining are detailed in *SI Appendix, Materials and Methods*. Metabolomics and glucose tracing experiments were performed at the Metabolomics Core at the University of Michigan and the sample preparation and procedures are detailed in *SI Appendix, Materials and Methods*.

**Data, Materials, and Software Availability.** All study data are included in the article and/or *SI Appendix*.

**ACKNOWLEDGMENTS.** We thank Dr. Janis Abkowitz (U of Washington) for providing the FLVCR1<sup>fl/fl</sup> mice, respectively, used in this study. This work was partly supported by NIH grant R01AI148289 (to C.-H.C.), R01NS120322 (to T.H.S.), F99AG079793 (to G.M.F.), and R01CA244931 (to C.A.L.).

Author affiliations: <sup>a</sup>Department of Microbiology and Immunology, University of Michigan Medical School, Ann Arbor, MI 48109; <sup>b</sup>Department of Biochemistry, Cell and Molecular Biology, West African Centre for Cell Biology of Infectious Pathogens, University of Ghana, Accra G4522, Ghana; <sup>c</sup>Department of Emergency Medicine, University of Michigan Medical School, Ann Arbor, MI 48109; <sup>d</sup>Rogel Cancer Center, University of Michigan Medical School, Ann Arbor, MI 48109; <sup>e</sup>Department of Nutritional Sciences, University of Michigan School of Public Health, Ann Arbor, MI 48109; <sup>f</sup>Department of Internal Medicine, Division of Gastroenterology and Hepatology, University of Michigan Medical School, Ann Arbor, MI 48109; and <sup>g</sup>Department of Molecular and Integrative Physiology, University of Michigan Medical School, Ann Arbor, MI 48109

Author contributions: A.K., C.Y., C.A.L., and C.-H.C. designed research; A.K., C.Y., A.N., T.D., G.M.F., P.S., and L.Z. performed research; T.H.S., C.A.L., and C.-H.C. contributed new reagents/analytic tools; A.K., C.Y., G.M.F., P.S., M.B.R., L.Z., O.Q., Y.-A.S., T.H.S., C.A.L., and C.-H.C. analyzed data; and A.K., C.Y., and C.-H.C. wrote the paper.

1. H. S. Azzam *et al.*, CD5 expression is developmentally regulated by T cell receptor (TCR) signals and TCR avidity. *J. Exp. Med.* **188**, 2301–2311 (1998).
2. I. Stefanova, J. R. Dorfman, R. N. Germain, Self-recognition promotes the foreign antigen sensitivity of naive T lymphocytes. *Nature* **420**, 429–434 (2002).
3. E. L. Yarosz *et al.*, Cutting edge: Activation-induced iron flux controls CD4 T cell proliferation by promoting proper IL-2R signaling and mitochondrial function. *J. Immunol.* **204**, 1708–1713 (2020).
4. Y. Lai *et al.*, Iron controls T helper cell pathogenicity by promoting glucose metabolism in autoimmune myopathy. *Clin. Transl. Med.* **12**, e999 (2022).
5. J. N. Frost *et al.*, Hepcidin-mediated hypoferrinemia disrupts immune responses to vaccination and infection. *Med* **2**, 164–179.e12 (2021).
6. C. Harding, J. Heuser, P. Stahl, Receptor-mediated endocytosis of transferrin and recycling of the transferrin receptor in rat reticulocytes. *J. Cell Biol.* **97**, 329–339 (1983).
7. M. Motamedi, L. Xu, S. Elahi, Correlation of transferrin receptor (CD71) with Ki67 expression on stimulated human and mouse T cells: The kinetics of expression of T cell activation markers. *J. Immunol. Methods* **437**, 43–52 (2016).
8. J. Arzes *et al.*, Non-transferrin-bound iron (NTBI) uptake by T lymphocytes: Evidence for the selective acquisition of oligomeric ferric citrate species. *PLoS One* **8**, e79870 (2013).
9. J. P. Pinto *et al.*, Physiological implications of NTBI uptake by T lymphocytes. *Front. Pharmacol.* **5**, 24 (2014).
10. H. h. Jabara *et al.*, A missense mutation in TFR2, encoding transferrin receptor 1, causes combined immunodeficiency. *Nat. Genet.* **48**, 74–78 (2016).
11. A. h. Aljohani *et al.*, Clinical and immunological characterization of combined immunodeficiency due to TFR2 mutation in eight patients. *J. Clin. Immunol.* **40**, 1103–1110 (2020).
12. A. Donovan *et al.*, Positional cloning of zebrafish ferroportin1 identifies a conserved vertebrate iron exporter. *Nature* **403**, 776–781 (2000).
13. G. Kovtunovych, M. A. Eckhaus, M. C. Ghosh, h. Ollivierre-Wilson, T. A. Rouault, Dysfunction of the heme recycling system in heme oxygenase 1-deficient mice: Effects on macrophage viability and tissue iron distribution. *Blood* **116**, 6054–6062 (2010).
14. G. Layer, J. Reichelt, D. Jahn, D. W. Heinz, Structure and function of enzymes in heme biosynthesis. *Protein Sci.* **19**, 1137–1161 (2010).
15. H. Atamna, D. W. Killilea, A. N. Killilea, B. N. Ames, Heme deficiency may be a factor in the mitochondrial and neuronal decay of aging. *Proc. Natl. Acad. Sci. U.S.A.* **99**, 14807–14812 (2002).
16. H. J. Kim, O. Khalimchuk, P. M. Smith, D. R. Winge, Structure, function, and assembly of heme centers in mitochondrial respiratory complexes. *Biochim. Biophys. Acta* **1823**, 1604–1616 (2012).
17. D. F. Bishop, A. S. Henderson, K. h. Astrin, Human delta-aminolevulinic synthase: Assignment of the housekeeping gene to 3p21 and the erythroid-specific gene to the X chromosome. *Genomics* **7**, 207–214 (1990).
18. A. A. Khan, J. G. Quigley, Heme and FLVCR-related transporter families SLC48 and SLC49. *Mol. Aspects Med.* **34**, 669–682 (2013).
19. A. A. Khan, J. G. Quigley, Control of intracellular heme levels: Heme transporters and heme oxygenases. *Biochim. Biophys. Acta* **1813**, 668–682 (2011).
20. S. K. Chiang, S. E. Chen, L. C. Chang, A dual role of heme oxygenase-1 in cancer cells. *Int. J. Mol. Sci.* **20**, 39 (2018).
21. P. Ponka, Tissue-specific regulation of iron metabolism and heme synthesis: Distinct control mechanisms in erythroid cells. *Blood* **89**, 1–25 (1997).
22. M. Philip *et al.*, Heme exporter FLVCR is required for T cell development and peripheral survival. *J. Immunol.* **194**, 1677–1685 (2015).
23. O. Stehling, R. Lill, The role of mitochondria in cellular iron-sulfur protein biogenesis: Mechanisms, connected processes, and diseases. *Cold Spring Harb. Perspect. Biol.* **5**, a011312 (2013).
24. A. Seguin *et al.*, The mitochondrial metal transporters mitoferrin1 and mitoferrin2 are required for liver regeneration and cell proliferation in mice. *J. Biol. Chem.* **295**, 11002–11020 (2020).
25. S. Dimeloe, A. V. Burgener, J. Grahert, C. Hess, T-cell metabolism governing activation, proliferation and differentiation; a modular view. *Immunology* **150**, 35–44 (2017).
26. L. A. Sena *et al.*, Mitochondria are required for antigen-specific T cell activation through reactive oxygen species signaling. *Immunity* **38**, 225–236 (2013).
27. B. U. Arafah *et al.*, Transphenoidal microsurgery in the treatment of acromegaly and gigantism. *J. Clin. Endocrinol. Metab.* **50**, 578–585 (1980).
28. A. W. El-Hattab, J. Suleiman, M. Almannai, F. Scaglia, Mitochondrial dynamics: Biological roles, molecular machinery, and related diseases. *Mol. Genet. Metab.* **125**, 315–321 (2018).
29. P. Bianco, "Mesenchymal" stem cells. *Annu. Rev. Cell Dev. Biol.* **30**, 677–704 (2014).
30. S. Merz, M. Hammermeister, K. Altmann, M. Durr, B. Westermann, Molecular machinery of mitochondrial dynamics in yeast. *Biol. Chem.* **388**, 917–926 (2007).
31. J. Bereiter-Hahn, M. Voth, Dynamics of mitochondria in living cells: Shape changes, dislocations, fusion, and fission of mitochondria. *Microsc. Res. Tech.* **27**, 198–219 (1994).
32. I. Bains, R. Antia, R. Callard, A. J. Yates, Quantifying the development of the peripheral naive CD4+ T-cell pool in humans. *Blood* **113**, 5480–5487 (2009).
33. C. Hong, M. A. Luckey, J. h. Park, Intrathymic IL-7: The where, when, and why of IL-7 signaling during T cell development. *Semin. Immunol.* **24**, 151–158 (2012).
34. J. Y. Park *et al.*, Soluble gamma cytokine receptor suppresses IL-15 signaling and impairs iNKT cell development in the thymus. *Sci. Rep.* **6**, 36962 (2016).
35. W. M. Zinzow-Kramer *et al.*, Strong basal/tonic TCR signals are associated with negative regulation of naive CD4(+) T cells. *Immunohorizons* **6**, 671–683 (2022).
36. Z. Wang *et al.*, Iron drives T helper cell pathogenicity by promoting RNA-binding protein PCBP1-mediated proinflammatory cytokine production. *Immunity* **49**, 80–92.e7 (2018).
37. A. Tarakhovskiy *et al.*, A role for CD5 in TCR-mediated signal transduction and thymocyte selection. *Science* **269**, 535–537 (1995).
38. M. J. Barnden, J. Allison, W. R. Heath, F. R. Carbone, Defective TCR expression in transgenic mice constructed using cDNA-based alpha- and beta-chain genes under the control of heterologous regulatory elements. *Immunol. Cell Biol.* **76**, 34–40 (1998).
39. J. M. Robertson, P. E. Jensen, B. D. Evavold, DO11.10 and OT-II T cells recognize a C-terminal ovalbumin 323–339 epitope. *J. Immunol.* **164**, 4706–4712 (2000).
40. J. Li *et al.*, Ferroptosis: Past, present and future. *Cell Death Dis.* **11**, 88 (2020).
41. A. Lawen, D. J. Lane, Mammalian iron homeostasis in health and disease: Uptake, storage, transport, and molecular mechanisms of action. *Antioxid. Redox Signal.* **18**, 2473–2507 (2013).
42. T. Hirayama, S. Kadota, M. Niwa, h. Nagasawa, A mitochondria-targeted fluorescent probe for selective detection of mitochondrial labile Fe(II). *Metalomics* **10**, 794–801 (2018).
43. Y. Wang, A. P. Landry, h. Ding, The mitochondrial outer membrane protein mitoNEET is a redox enzyme catalyzing electron transfer from FMNH(2) to oxygen or ubiquinone. *J. Biol. Chem.* **292**, 10061–10067 (2017).
44. L. Tilokani, S. Nagashima, V. Paupé, J. Prudent, Mitochondrial dynamics: Overview of molecular mechanisms. *Essays Biochem.* **62**, 341–360 (2018).
45. Q. Zheng *et al.*, Iron overload promotes mitochondrial fragmentation in mesenchymal stromal cells from myelodysplastic syndrome patients through activation of the AMPK/MFF/Drp1 pathway. *Cell Death Dis.* **9**, 515 (2018).
46. M. D. Buck *et al.*, Mitochondrial dynamics controls T cell fate through metabolic programming. *Cell* **166**, 63–76 (2016).
47. C. R. Chang *et al.*, A lethal de novo mutation in the middle domain of the dynamin-related GTPase Drp1 impairs higher order assembly and mitochondrial division. *J. Biol. Chem.* **285**, 32494–32503 (2010).
48. F. Baizauli *et al.*, Mitochondrial respiration controls lysosomal function during inflammatory T cell responses. *Cell Metab.* **22**, 485–498 (2015).
49. M. Nakaya *et al.*, Inflammatory T cell responses rely on amino acid transporter ASCT2 facilitation of glutamine uptake and mTORC1 kinase activation. *Immunity* **40**, 692–705 (2014).
50. D. W. Scott, T. S. Dunn, M. E. Ballestas, S. h. Litovsky, R. P. Patel, Identification of a high-mannose ICAM-1 glycoform: Effects of ICAM-1 hypoglycosylation on monocyte adhesion and outside in signaling. *Am. J. Physiol. Cell Physiol.* **305**, C228–C237 (2013).
51. R. D. Cummings, S. Kornfeld, Characterization of the structural determinants required for the high affinity interaction of asparagine-linked oligosaccharides with immobilized Phaseolus vulgaris leucoagglutinating and erythroagglutinating lectins. *J. Biol. Chem.* **257**, 11230–11234 (1982).
52. M. E. Brinkner, D. B. Friedman, C. G. Cigarroa, P. A. Grayburn, Relation of thrombus in the left atrial appendage by transesophageal echocardiography to clinical risk factors for thrombus formation. *Am. J. Cardiol.* **74**, 391–393 (1994).
53. K. Voss *et al.*, Elevated transferrin receptor impairs T cell metabolism and function in systemic lupus erythematosus. *Sci. Immunol.* **8**, eabq0178 (2023).
54. S. P. Persaud, C. R. Parker, W. L. Lo, K. S. Weber, P. M. Allen, Intrinsic CD4+ T cell sensitivity and response to a pathogen are set and sustained by avidity for thymic and peripheral complexes of self peptide and MHC. *Nat. Immunol.* **15**, 266–274 (2014).
55. G. Bronfort, M. Haas, R. Evans, B. Leininger, J. Triano, Effectiveness of manual therapies: The UK evidence report. *Chiropr. Osteopat.* **18**, 3 (2010).
56. A. A. V. Milam *et al.*, Tonic TCR signaling inversely regulates the basal metabolism of CD4(+) T cells. *Immunohorizons* **4**, 485–497 (2020).
57. W. Ouyang, O. Beckett, R. A. Flavell, M. O. Li, An essential role of the Forkhead-box transcription factor Foxo1 in control of T cell homeostasis and tolerance. *Immunity* **30**, 358–371 (2009).
58. J. A. Wofford, h. L. Wieman, S. R. Jacobs, Y. Zhao, J. C. Rathmell, IL-7 promotes Glut1 trafficking and glucose uptake via STAT5-mediated activation of Akt to support T-cell survival. *Blood* **111**, 2101–2111 (2008).
59. C. Wiel *et al.*, BACH1 stabilization by antioxidants stimulates lung cancer metastasis. *Cell* **178**, 330–345.e22 (2019).
60. H. Suzuki *et al.*, Heme regulates gene expression by triggering Crm1-dependent nuclear export of Bach1. *EMBO J.* **23**, 2544–2553 (2004).
61. M. Watanabe-Matsui *et al.*, Heme regulates B-cell differentiation, antibody class switch, and heme oxygenase-1 expression in B cells as a ligand of Bach2. *Blood* **117**, 5438–5448 (2011).
62. S. Tsukumo *et al.*, Bach2 maintains T cells in a naive state by suppressing effector memory-related genes. *Proc. Natl. Acad. Sci. U.S.A.* **110**, 10735–10740 (2013).
63. V. Fiorito *et al.*, The heme synthesis-export system regulates the tricarboxylic acid cycle flux and oxidative phosphorylation. *Cell Rep.* **35**, 109252 (2021).
64. F. Vinchi *et al.*, Heme exporter FLVCR1a regulates heme synthesis and degradation and controls activity of cytochromes P450. *Gastroenterology* **146**, 1325–1338 (2014).
65. D. Chiabrando *et al.*, The mitochondrial heme exporter FLVCR1b mediates erythroid differentiation. *J. Clin. Invest.* **122**, 4569–4579 (2012).
66. X. Tang *et al.*, Heme oxygenase-1 increases intracellular iron storage and suppresses inflammatory response of macrophages by inhibiting M1 polarization. *Metalomics* **15**, mfad062 (2023).
67. D. M. Ward, S. M. Cloonan, Mitochondrial iron in human health and disease. *Annu. Rev. Physiol.* **81**, 453–482 (2019).
68. A. D. Sheftel, A. S. Zhang, C. Brown, O. S. Shirihai, P. Ponka, Direct interorganellar transfer of iron from endosome to mitochondrion. *Blood* **110**, 125–132 (2007).
69. S. E. Wiley, A. N. Murphy, S. A. Ross, P. van der Geer, J. E. Dixon, MitoNEET is an iron-containing outer mitochondrial membrane protein that regulates oxidative capacity. *Proc. Natl. Acad. Sci. U.S.A.* **104**, 5318–5323 (2007).
70. J. Schlesier, M. Rohde, S. Gerhardt, O. Einsle, A conformational switch triggers nitrogenase protection from oxygen damage by Shethna protein II (FeSII). *J. Am. Chem. Soc.* **138**, 239–247 (2016).
71. R. J. DeBerardinis, J. J. Lum, G. Hatzivassiliou, C. B. Thompson, The biology of cancer: Metabolic reprogramming fuels cell growth and proliferation. *Cell Metab.* **7**, 11–20 (2008).
72. Y. Shen *et al.*, Metabolic control of the scaffold protein TK55 in tissue-invasive, proinflammatory T cells. *Nat. Immunol.* **18**, 1025–1034 (2017).